XL CILAMCE
IBERO-LATIN AMERICAN CONGRESS ON COMPUTATIONAL METHODS IN ENGINEERING
NOVEMBER 11-14, 2019
Praiamar Natal Hotel & Convention
Natal, RN-BRAZIL

THERMOELECTRIC POWER PLANT PERFORMANCE AND EMISSION CONTROL SIMULATION

Bárbara A. P. C. Ferro
barbara_cv_ferro@hotmail.com
UFGD
Rod. Dourados-Itahum, km 12, C. Universitária, Cx. Postal 364, CEP 79804-970, Dourados/MS, Brazil
Ricardo A. V. Ramos
ricardo.ramos@unesp.br
IPBEN-FEIS/UNESP
Avenida Brasil, 56 - Centro, CEP 15385-000, Ilha Solteira/SP, Brazil
Augusto S. Bornschlegell
augustosalomao@ufgd.edu.br
UFGD
Rod. Dourados-Itahum, km 12, C. Universitária, Cx. Postal 364, CEP 79804-970, Dourados/MS, Brazil

Abstract. Energy is undoubtedly a subject that concerns the government and society. In addition to the economic liability, the environmental aspects are equally important. A thermoelectric power plant is a solution that fulfill both requirements. The present work evaluated the composition of the combustion products of a thermoelectric power plant through an analytic and numerical models. The main polluent components found in the methane combustion products are CO_X, SO_X, NO_X and solid particles. Regarding the ozone formation, the NO_X is the most harmful combustion product. Brayton's thermodynamic cycle, including combustion, was numerically modelled and implemented through Scilab© routines. The input data was based on real power plant operation conditions, which the compressor isotropic process, the compression rate, the air and fuel mass rates, the combustion chamber and gas turbine's efficiency are known. The combustion reaction methodology takes into account the equilibrium constants, as proposed in the literature. The combustion products concentration were then evaluated as they flow through the turbine and are released to the atmospheric conditions. The chemFoam solver of the OpenFOAM software was used in order to compare the combustion product's concentrations obtained with the proposed model. In addition, the results from the combustion model were compared with the equivalent air (ideal gas) model, without combustion. The difference in thermal efficiency estimation was approximately of 28 %.

Keywords: Thermal Power Plant, Combustion, Gas Cycle.

1 Introduction

The electric energy supply expansion and its demand bring a relevant concern to both the government and society. The perspective of the Brazilian and the world's electric expansion indicates that natural gas and the renewable sources are rising. This is a chance of diversification of the Brazilian's electric system leading to an independent path from the hydroelectric plants. However, it should be pointed out that thermoelectric plants demand a more complex operation system than the hydroelectric ones due to high temperatures and high pressures of the working fluid.

Investments on natural gas based thermoelectric power plants is one of the alternatives for increasing the electric energy production. Throughout the conversion of the fuel's energy to electric energy, these plants have a similar working method no matter the fuel used. The efficiency of a standard unit is low, typically around 30 to 40 % according to Lora *et al*. [1]. For this reason, an interesting optimization idea is to rise this percentage by means of a cogeneration setup. A standard unit is composed of a gas turbine, a heat recovery boiler and a steam turbine.

A gas turbine is a thermal machine which working fluid is the air. The working fluid is accelerated as it passes through the turbine, in other words, it has its kinetic energy increased. Also, the air must have its pressure increased and heat must be injected. The resulting energy (enthalpy increase) turns into power on the turbine's shaft. The exaust residual gas heat is usually absorved by a Heat Recovery Steam Generators (HRSG) boiler, where the remaining steam is directed to a steam turbine in order to run an electric generator.

The main advantage of this process is the cost reduction. This is only possible due to the maximum conversion of the energy's source. The system thermal efficiency can reach 85 %, including polluent emisson reduction, according to Lora *et al*. [1]. It is worth mention that the main concerns related to thermoelectric generation are the emissions that causes the greenhouse effect. The components found on the exaust port of the gas turbine are mainly hydrocarbons, carbon oxide, nitrogen oxide, sulphur oxide and the remaining solid particles from the fuel's incomplete combustion and from air particles. Among them, the NO_X is the most harmfull because of its inhibition to the ozone formation.

The Brayton's cycle classical approach does not take into account the combustion reaction. The most common modelling method evolves a standard air analysis, where the working fluid is modeled as air in the whole cycle. In this modelling, the temperature increase is due heat transfer from an external source. The proposed methodology in this work aims to deal with the combustion process modelling and its resulting performance indicators. Therefore, in this work, the objective is to evaluate the combustion gases behavior on a Brayton's cycle process.

The obtained values will be compared with the simulation considering the air based model. The combustion products composition that will be released to the atmosphere are compared with a second numerical model based on the chemFoam solver from the OpenFOAM software.

2 Mathematical Modelling

Brayton's thermodinamic cycle, including combustion, is numerically modelled and implemented on Scilab© routines. This thermal modelling was elaborated as close as possible to the real conditions. For the sake of simplicity, some premisses were adopted, they are:

· The fluid velocity and head losses were not considered;

· Each analysed component is a control volume under permanent regime;

· The compressor and the turbine are considered adiabatic;

The input data was established according to the operational conditions of a Thermoelectric power plant studied by Branco [2] on Table 1. These values include the compressor isotropic efficiency (η_{cp}), the compression rate (r_{cp}), the air mass flow rate ($\dot{m}_{ar}$), the gas mass flow rate ($\dot{m}_{comb}$), the combustion chamber efficiency (η_{cb}) and the turbine isotropic efficiency (η_{tg}). The employed pressure (P_1) and temperature (T_1) values are the standard ones (T=298 K, P=101.325 kPa).

Table 1. Input data from Branco [2] considered to evaluate the gas cycle.

Input	Value
Compressor isentropic efficiency (η_{cp})	87.0 %
Turbine isentropic efficiency (η_{tg})	92.0 %
Combustion chamber efficiency (η_{cb})	90.0 %
Compression ratio (r_{cp})	14.5
Air mass flow ($\dot{m}_{ar}$)	197.5 kg / s
Combustion products exaust mass flow ($\dot{m}_{ex}$)	202.2 kg / s
Fuel mass flow ($\dot{m}_{comb}$)	4.71 kg / s

The methodology is composed by three models: the air based model (Case I), a combustion model taking into account chemical equilibrium (Case II) and a combustion model considering chemical kinetics (Case III). The Brayton's cycle matrix base model complies compressor, combustion chamber and the gas turbine (Fig. 1).

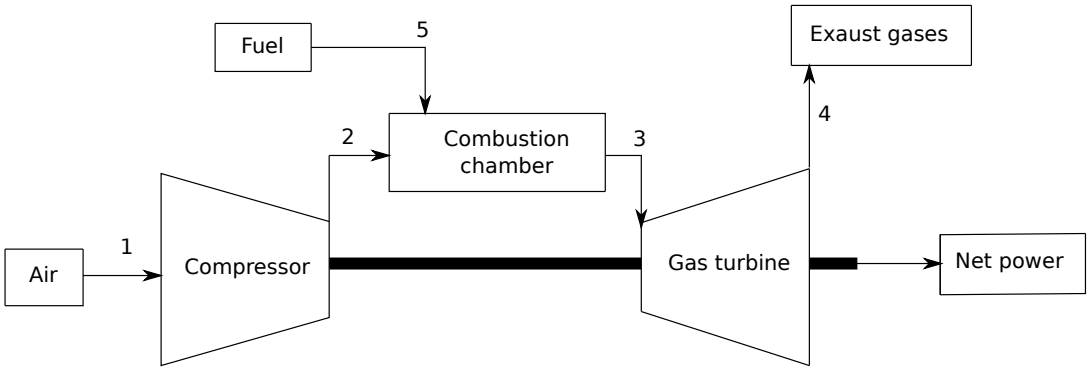

Figure 1. Brayton's cycle diagram (From Queiroz and Matias [3]).

All of the formulations referring to these items were established and developed considering the irreversibility effects.

2.1 Brayton's cycle with no combustion - Case I

The isentropic Brayton cycle behavior (1-2s-3-4s), as well the one the includes the compressor and gas turbine irreversibilities (1-2-3-4) are shown in Fig. 2, where it is possible to note the influence of the losses on the compression and expansion processes.

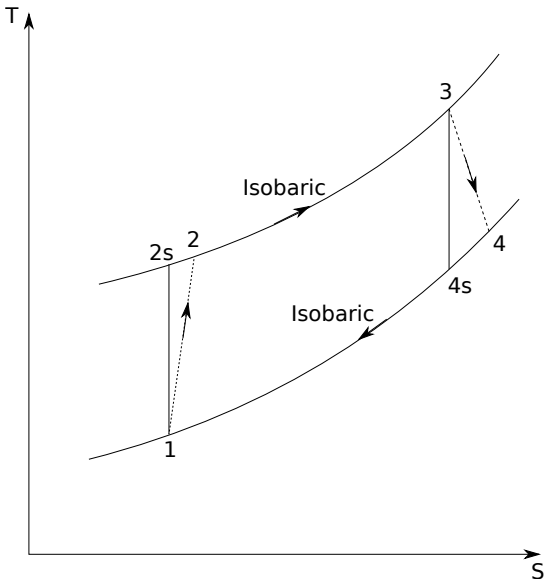

Figure 2. Brayton cycle temperature-entropy diagram, adapted from Lora *et al*. [1].

In order to initiate the fluid's thermodynamic modelling, air is defined as 21 % of oxygen and 79 % of nitrogen, so that, for each mole of O_2, there are 3.76 moles of N_2. The total number of moles on the mixture, N, is defined by:

$$N = \sum_{i=1}^{n} n_i \tag{1}$$

The molar fraction, y_i, is given by the number of moles divided by the total number of moles of the mixture. The mixture molar mass, M (g/mol), is given by the sum of the molar mass of each product, m (g/mol), multiplied by the molar fraction of the mixture.

$$M = \sum_{i=1}^{n} y_i \, m \tag{2}$$

The ideal gas constant for the mixture, R (kJ/K) is related to the universal gas constant, Ru (8.314 kJ/kmol K), by:

$$R = \frac{Ru}{M} \tag{3}$$

Based on the preavious definitions, the combustion products (mixture) thermodynamic properties, as the molar entropy of the i mixture component, $\bar{s}_i$ (kJ/kmol K), is defined as:

$$\bar{s}_i(T, P) = \bar{s}_i{}^o(T) - Ru \; ln(P_i/P_o) \tag{4}$$

where, $\bar{s}_i{}^o$ is the formation entropy, (kJ/(kmol K)), P_o is the atmospheric pressure (101.325 kPa) and P_i is the partial pressure defined as the product of the molar fraction (y_i) and the mixture's pressure (kPa). The molar entropy of each mixture component i is given by Eq. (5).

$$\bar{s_i}^o \;=\; R_u \left(a_1 lnT + a_2 T + \frac{a_3}{2} T^2 + \frac{a_4}{3} T^3 + \frac{a_5}{4} T^4 + a_7 \right) \tag{5}$$

The coefficient values (a_i) of the property curve fitting are based on $JANAF\ Thermochemical\ Tables$ and compiled at Ferguson and Kirkpatrick [4]. Lastly, the mixture's entropy, s (kJ/kg k) is the sum of the molar entropy of each mixture component multiplied by its relative molar fraction, as presented in Eq. (6):

$$s \;=\; \frac{1}{M} \sum \bar{s_i}\, y_i \tag{6}$$

Following the same approach, the molar enthalpy of the i mixture component is given by Eq. (7) and the mixture's enthalpy (kJ/kg) is defined on Eq. (8).

$$\bar{h_i} \;=\; R_u T \left(a_1 + \frac{a_2}{2} T + \frac{a_3}{3} T^2 + \frac{a_4}{4} T^3 + \frac{a_5}{5} T^4 + \frac{a_6}{T} \right) \tag{7}$$

$$h \;=\; \frac{1}{M} \sum \bar{h}_i y_i \tag{8}$$

The compressor exit pressure (P_2) can be calculated by:

$$P_2 = r_{cp} P_1 \tag{9}$$

As an isotropic process, the second state isotropic entropy (s_{2s}) is considered the same as the first state's entropy (s_1), therefore, the theoretical temperature for the second state (T_{2s}) is defined. To calculate the temperature value, an iterative method is necessary. From an arbitrary temperature guess, the iterative process ilustrated in Fig. 3 returns a temperature value for which the isotropic process could be satisfied. The implemented iteractive algorithm is based on the Newton–Raphson's method, which calculates the the target function derivative in order to correct the preavious temperature guess. The process is repeated until a value that respect the imposed numerical tolerance is reached.

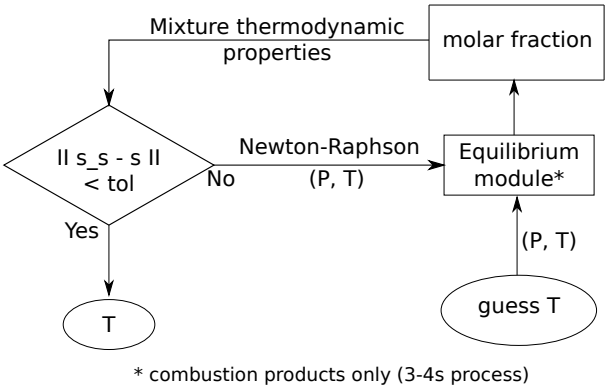

Figure 3. Iterative algorithm to calculate thermodynamic properties in isoentropic processes.

From T_{2s}, it is possible to obtain the theoretical enthalpy's values for this point (h_{2s}). Based on the compressor's isotropic efficiency it can be found the state 2 real enthalpy h_2 through Eq. (10).

$$\eta_{cp} = \frac{h_1 - h_{2s}}{h_1 - h_2} \tag{10}$$

From (h_2), (T_2) can be found following the same reasoning from Fig. 3. Thus, the second state is defined and all the corresponding thermodynamics properties can be calculated.

Part of the losses occurred in the combustion chamber were accounted considering its efficiency (η_{cb}). The injected fuel (methane) chemical energy, (kJ), is given by Eq. (11).

$$\dot{Q}_{comb} = \dot{m}_{comb} LHV \tag{11}$$

Where , LHV refers to the fuel Lower Heating Value ($50.019,93\ kJ/kg$). The energy balance at the combustion chamber can be described as demonstrated in Ziółkowski *et al.* [5] and presented in Eq. (12). The h_{comb} value is based on the air properties.

$$h_{3i} = \frac{\eta_{cb}\left(\dot{Q}_{comb} + \dot{m}_{ar} h_2 + \dot{m}_{comb} h_{comb}\right)}{\dot{m}_{ex}} \tag{12}$$

In a first approach, the 3-4 process in the turbine is considered as isotropic and its expansion as ideal. Just like the second state definition, the fourth state's entropy (s_4) is obtained by an iteractive process. The corresponding temperature is obtained through the thermal efficience definition in Eq. (13).

$$\eta_{tg} = \frac{h_3 - h_4}{h_3 - h_{4s}} \tag{13}$$

The thermal efficiency, when combustion is modeled as Ziółkowski *et al.* ([5]), is defined by Eq. (14):

$$\eta_I = \frac{\dot{W}_t - \dot{W}_c}{\dot{Q}_{comb}} \tag{14}$$

Where, $\dot{W}_t$ is the work produced by the turbine (kJ/s) and $\dot{W}_c$ is the necessary work (kJ/s) to run the compressor. They are calculated through the isotropic efficiency values of the turbine (Eq. (15)) and the compressor (Eq. (16)), respectively. The difference between the produced and used work is the cycle's liquid work ($\dot{W}_{cycle} = \dot{W}_t - \dot{W}_c$).

$$\dot{W}_t = \eta_{tg} \dot{m}_{ex} (h_3 - h_{4s}) \tag{15}$$

$$\dot{W}_c = \frac{\dot{m}_{ar}(h_{2s} - h_1)}{\eta_{cp}} \tag{16}$$

The cycle reverse work rate, which is the fraction of the turbine work used to run the compressor, is given by Eq. (17):

$$bwr = \frac{\dot{W}_c}{\dot{W}_t} \tag{17}$$

2.2 Brayton's cycle including combustion modelling using equilibrium contants- Case II

The used methodology to quantify the products of combustion is based on the method of the equilibrium constants applied by Olikara and Borman [6] and Ferguson and Kirkpatrick [4] to the gas phase products of the hydrocarbons' combustion. For the present reactions modelling, 10 significant products species are considered, as presented in Eq. (18).

$$C_aH_bO_cN_d + \frac{as}{\phi}\left(O_2 + 3,76N_2\right) \rightarrow n_1CO_2 + n_2H_2O + n_3N_2 + n_4O_2 + n_5CO + n_6H_2 + n_7H + n_8O + OH + n_{10}NO \tag{18}$$

Where as is the stoichiometric fuel-air rate and ϕ is the equivalence ratio, defined as:

$$\phi = \frac{FA}{FA_s} \tag{19}$$

Where FA is the fuel-air actual ratio and FA_s is the air-fuel stoichiometric ratio. If ϕ <1 the mixture is poor, ϕ >1 defines a rich mixture and ϕ = 1 a stoichiometric one. For the present model, we considered ϕ = 0.80.

The mass conversion principle is defined by Eq. (20) and the gas phase equilibrium equation are described on Eq. (21). In the equilibrium equations there are the hydrogen, oxygen, air and carbon dioxide's dissociation, and the formation of OH and NO.

$$\begin{aligned}
C &: a = (y_1 + y_5)\,N \\
H &: b = (2y_2 + 2y_6 + y_7 + y_9)\,N \\
O &: c + 2\frac{as}{\phi} = (2y_1 + y_2 + 2y_4 + y_5 + y_8 + y_9 + y_{10})\,N \\
N &: d + 7.52\frac{as}{\phi} = (2y_3 + y_{10})\,N
\end{aligned} \tag{20}$$

$$\begin{aligned}
\frac{1}{2}H_2 &\rightleftharpoons H \quad K_1 = \frac{y_7 P^{1/2}}{y_6^{1/2}} \\
\frac{1}{2}O_2 &\rightleftharpoons O \quad K_2 = \frac{y_8 P^{1/2}}{y_4^{1/2}} \\
\frac{1}{2}H_2 + \frac{1}{2}O_2 &\rightleftharpoons OH \quad K_3 = \frac{y_9}{y_4^{1/2} y_6^{1/2}} \\
\frac{1}{2}N_2 + \frac{1}{2}O_2 &\rightleftharpoons NO \quad K_4 = \frac{y_{10}}{y_4^{1/2} y_3^{1/2}} \\
H_2 + \frac{1}{2}O_2 &\rightleftharpoons H_2O \quad K_5 = \frac{y_2}{y_4^{1/2} y_6 P^{1/2}} \\
CO + \frac{1}{2}O_2 &\rightleftharpoons CO_2 \quad K_6 = \frac{y_1}{y_4^{1/2} y_5 P^{1/2}}
\end{aligned} \tag{21}$$

The equilibrium constants K_i(T) regression curve is based on $JANAF\ Thermochemical\ Tables$, between the temperatures of 600 < T < 4000 K, as described by Ferguson and Kirkpatrick [4]. Equations

20 and 21 form a set of 10 variables and 10 non-linear equations. Robust algorithms shall be used to solve this highly non-linear system. We employed the so called Newton-Reduced method, which evaluates if Newton full step assures a descent (minimization problem) direction. If not, half step is considered and so forth until a pre-stablished tolerance is achieved.

2.3 Algorithm overview

The whole cycle algorithm is presented in Fig. 4.

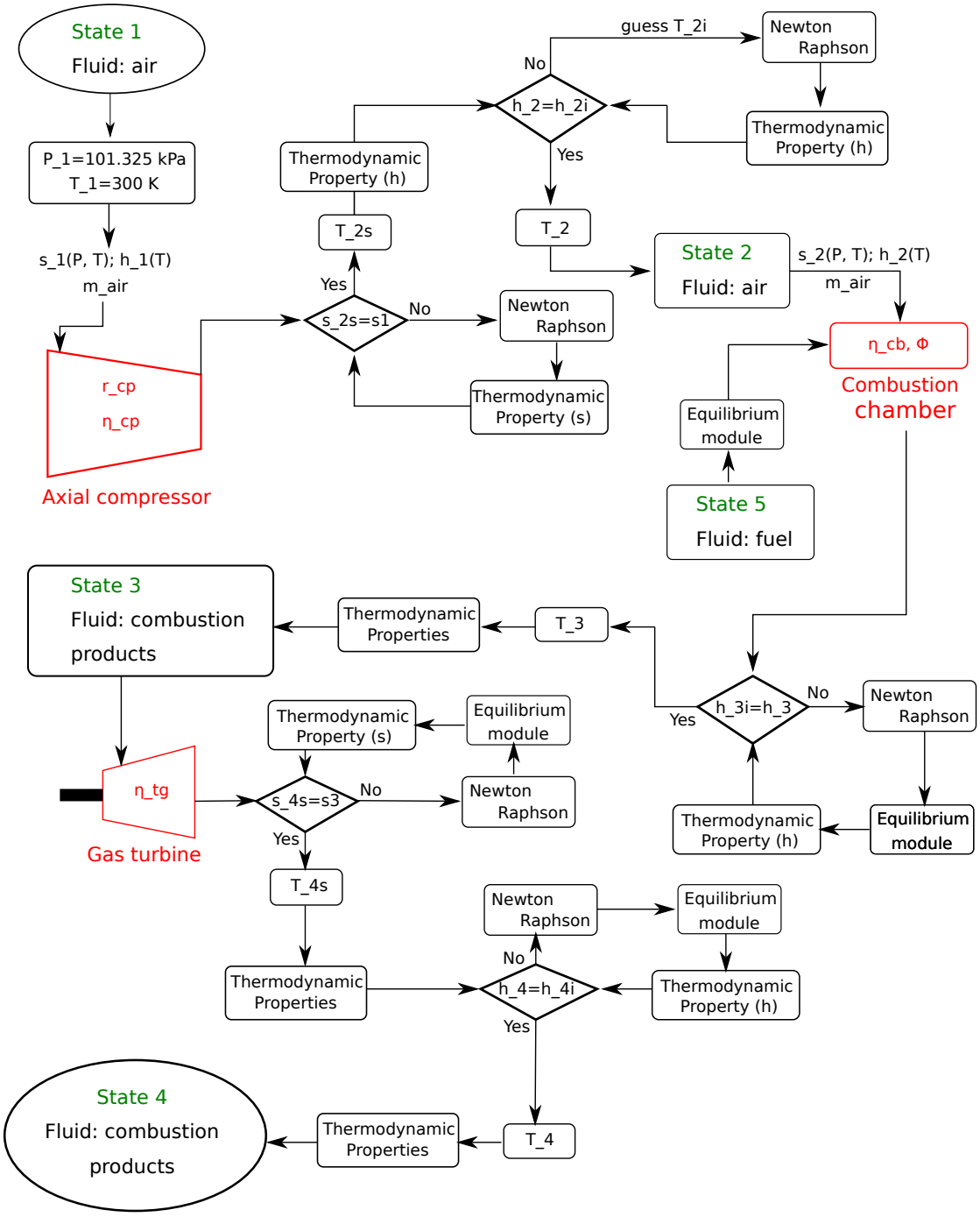

Figure 4. Brayton's cycle with combustion modelling algorithm.

2.4 Chemical kinetics of the combustion chamber

In order to compare different methodologies, it was used the combustion solver from the OpenFOAM software (Open Field Operation And Manipulation) which is an open source code composed by modules written in $C++$. According to Maioli *et al.* [7], the solvers treat the equations through specific methodologies for each case. These cases follow an structure of directories that have archives with the necessary information to simulate the specified case, with the problems' parameters such as the physical properties and numerical methods.

The empoyed combustion solver was the chemFoam, a chemistry related simulator based on the chemical kinetics of the methane's combustion. The gri tutorial was used as a basis case. The reaction's rate is modelled by the Arrhenius' equation, considering 325 reactions for this fuel.

In this model, the reactions are considered reversible ($reversibleArrheniusReaction$), by other words, the reactions can happen in forward direction (reagents forming products) or backwards. The chemical equilibrium is reached when the forward and backwards reaction's rates are the same. The thermodynamics properties evaluation in OpenFOAM is based on $JANAF\ Thermochemical\ Tables$. After the simulation, the reagents and products' molar fraction variation through time are obtained.

3 Results

3.1 Comparison between the models with combustion and without combustion

Thermodynamics analysis was carried out for each gas cycle equipment. Thermal efficiency, cycle net power and the reverse work ratio for Case I (pure air) and Case II (equilibrium modelling) are presented in Table 2.

Table 2. Pure air vs. combustion modelling.

Parameter	Case I	Case II
η_I	30.62 %	58.86 %
bwr	39.75 %	25.39 %
$\dot{W}_{ciclo}/\dot{m}$	351.43 kJ/kg	681.39 kJ/kg

The thermal usual efficiencies according to Moran *et al.* [8] and Lora *et al.* [1] are, respectively, of 28.24 and 27.66 %. The bwr usual values, according to Moran *et al.* [8], are between 40 and 80 %. The results sugests that chemical transport through pure air is not as effective as the products mixture. Some irreversibilities associated to combustion were also not take into account, as the air-fuel pre-mixing and chamber geometry, which have great impact on the reaction's efficiency.

The temperature versus entropy diagrams containig the cycle irreversibilities of Case I and II are presented in Fig. 5 and 6 respectivelly. The dashed curved lines represent the isobaric lines. Since in Case I it is modelled pure air, the 2-3 process (from state 2 to 3) can be represented throughout.

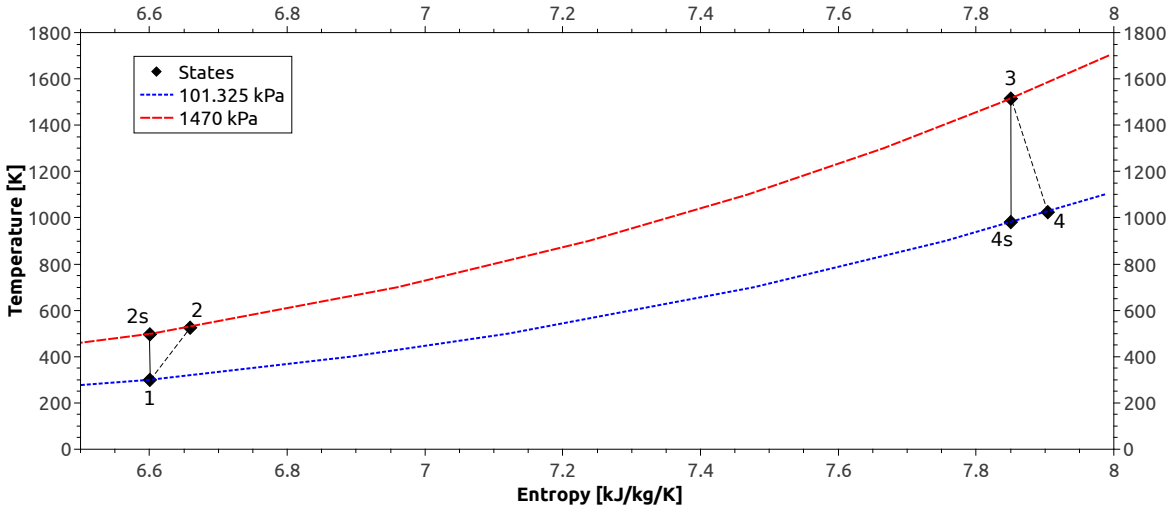

Figure 5. Temperature-entropy diagram with no combustion modelling.

The isobaric line equivalent to the 2-3 process in Case II starts at the auto ingnition temperature point, since it is assumed that combustion is maintained from that point. The auto ignition temperature is aproximately 840 [K], according to CETESB [9] and Gama [10]. Below this value, without any activation energy source, the gases can be modelled as a fuel-air mixture. Then, only the combustion products are represented in the 1470 kPa isobaric line in Fig. 6. The 101.325 kPa isobaric line is not fully represented due convergence issues. The thermodynamic properties estimation at lower temperatures are also limitated by the $JANAF\ \ Thermochemical\ Tables$ polynomial regression available at Ferguson and Kirkpatrick [4].

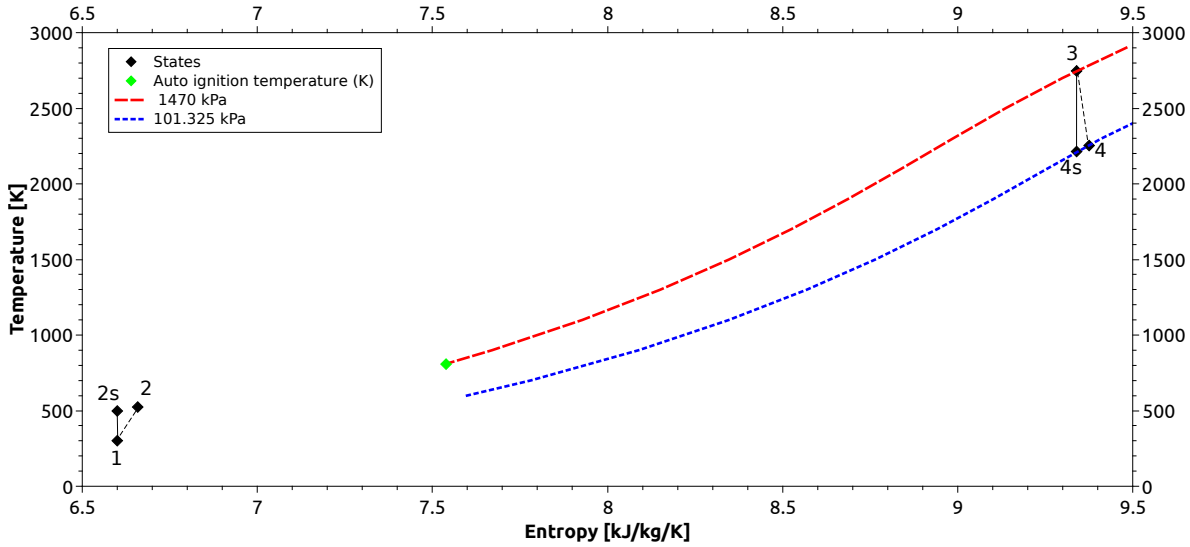

Figure 6. Temperature-entropy diagram with combustion modelling.

In both cases, the states 1 and 2 are identical, since the combustion reaction occurs at the 2-3 process. At state 3, the model considering combustion (Case II) presents entropy 15.9 % higher than Case I. Similarly, in state 4, entropy in Case II is 15.7 % higher than in Case I.

3.2 Chemical kinetics model

The molar fraction from the equilibrium model (Case II) and the kinetics model (Case III) are compared and presented in Table 3.

Table 3. Combustion products molar fraction.

Component	Chemical kinetics	Chemical equilibrium	Difference (%)
CO_2	0.116647	0.0738652	36.67
H_2O	0.0975562	0.1505664	35.21
N_2	0.728234	0.7227036	0.76
O_2	0.0401944	0.0363880	9.47
CO	0.0037032	0.0033376	9.87
H_2	8.81091x10^{-5}	0.0012650	-
H	8.08072x10^{-6}	0.0002709	-
O	0.000394833	0.0007218	45.29
OH	0.0034788	0.0048772	28.67
NO	0.009655939	0.0060042	37.81

The differences in molar fractions goes from 0.8 to 45.4 %. The highest diferences correspond to the H_2 and H components. Numerically, their levels are virtually null when comparing with the complementary elements in Case III (kinetics model). It means that those elements were, in Case III, recombined to form other elements that are not covered in the equilibrium model. For instance, in Case III there are 37 components with hidrogen whereas there are only 4 in the Case II model. Excluding water, there is no relevant hidrogen compound in the kinetics modeling (Fig. 7).

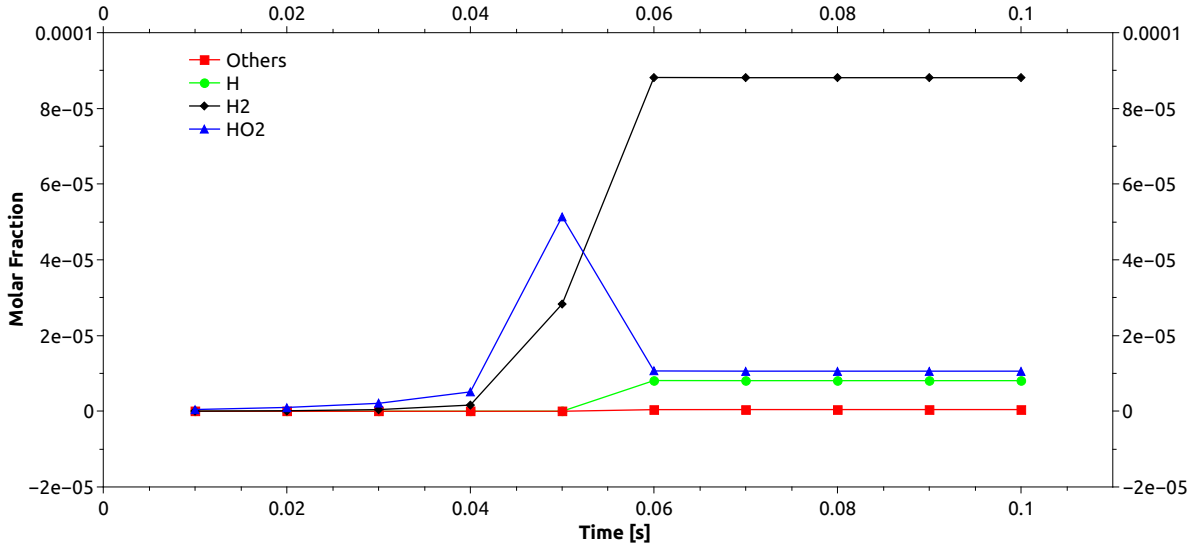

Figure 7. Chemical reactions regarding hidrogen.

The chemical kinetics can be evaluated over time in Figure 8. The combustion reaction accurs in 0.01 second. This is the required time to the mixture react and attain chemical equilibrium. In this

interval, temperature increases from 1000 to 2500 [K].

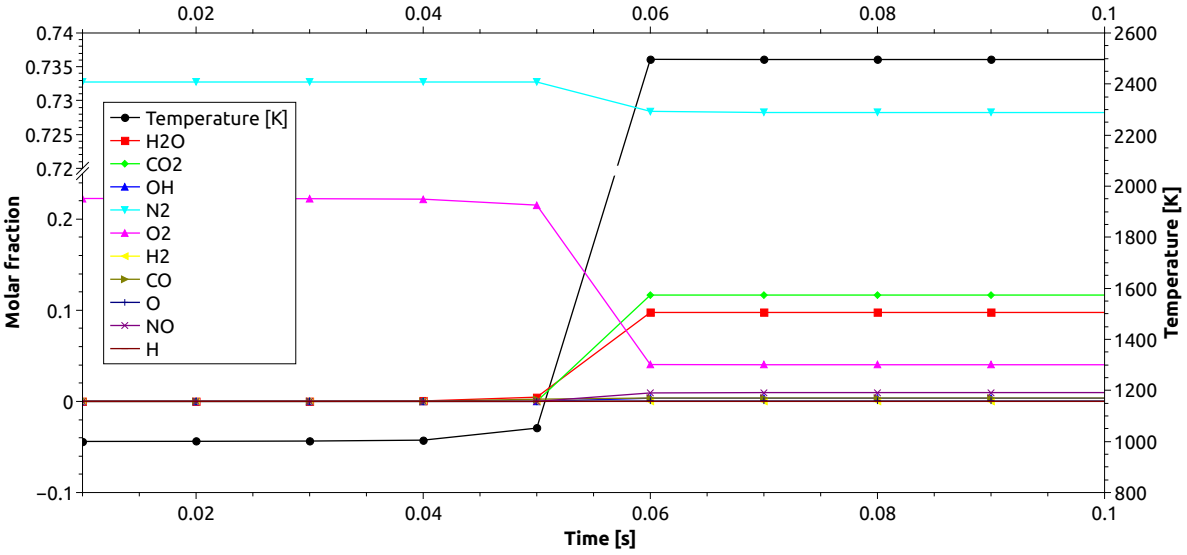

Figure 8. Chemical reaction inside the combustion chamber.

In the equilibrium model (Case II), the obtained temperature is 2745 [K], 8.9 % higher than in Case III.

The fuel composition, the combustion chamber project and operating parameters are variables that causes variation in the NO_X concentrations in the exaust pipe. NO_X are represented by the sum of NO (nitric oxide) and NO_2 (nitric dioxide). It is observed that a small quantity of N_2 decreases during the reaction forming the NO_X.

The carbon monoxide (CO) is formed during incomplete combustion, resultig in energy loss and atmospheric pollution. The presence of O_2 (in excess) all over the combustion chamber is important to form CO_2 instead of CO. In another hand, the NO_X formation is induced in the presence of O_2. Then, a compromisse is required to balance both polluents quantities.

Table 4 presents the emission values for NO and CO for both Cases (II and III). The concentrations calculation procedure was based in [11].

Table 4. NO and CO concentrations.

Parameter	NO		CO	
	Chemical Eq.	Kinetics Eq.	Chemical Eq.	Kinetics Eq.
Molar Fraction	0.0060042	0.0107036	0.0039292	0.0041035
Molar concentration (mg/mol)	0.2762	0.4924	0.11005	0.11491
Concentration (mg/(Nm^3)	12.3238	21.9975	4.9102	5.1280
Concentration (ppm)	9.324	16.65	3.981	4.158

The local regulatory authority (CONAMA) defines the atmospheric polluents emission limits for turbines employed in electrical energy generation. It applies for natural gas and liquid fuels based turbines, simple or combined cycles. For gas turbines with net power less than 100 [MW] operating with natural gas, the NO_X concentration limit is 90 [mg/(Nm)^3] and the CO concentration limit is 65 [mg/(Nm)^3] .

As presented in Table 4 and in Figures 9 and 10 the polluent concentrations estimated are below

the emission limits defined at [11].

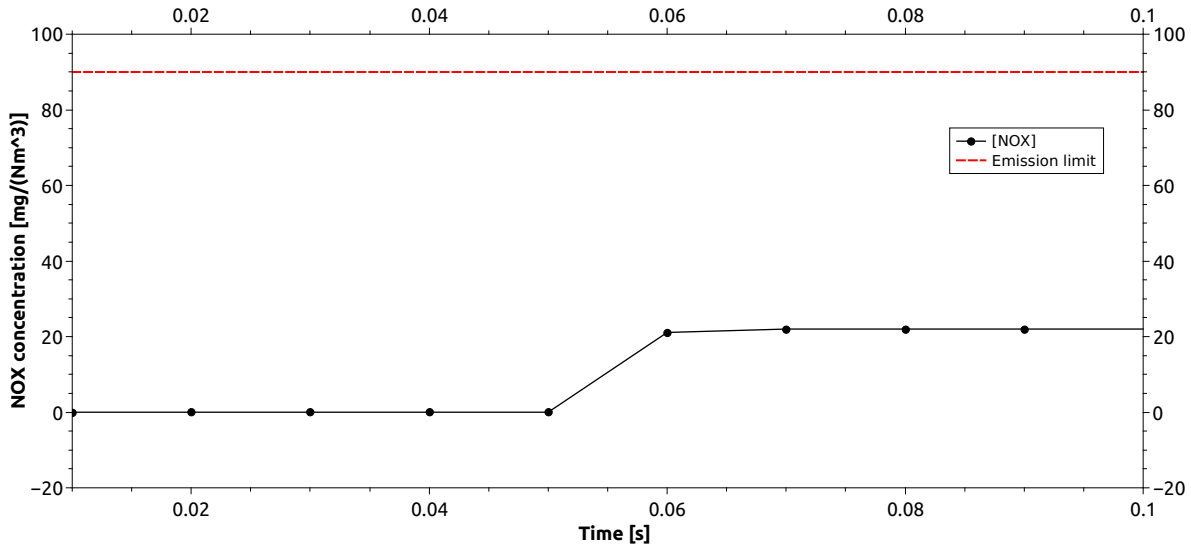

Figure 9. NO_X concentration during the combustion reaction.

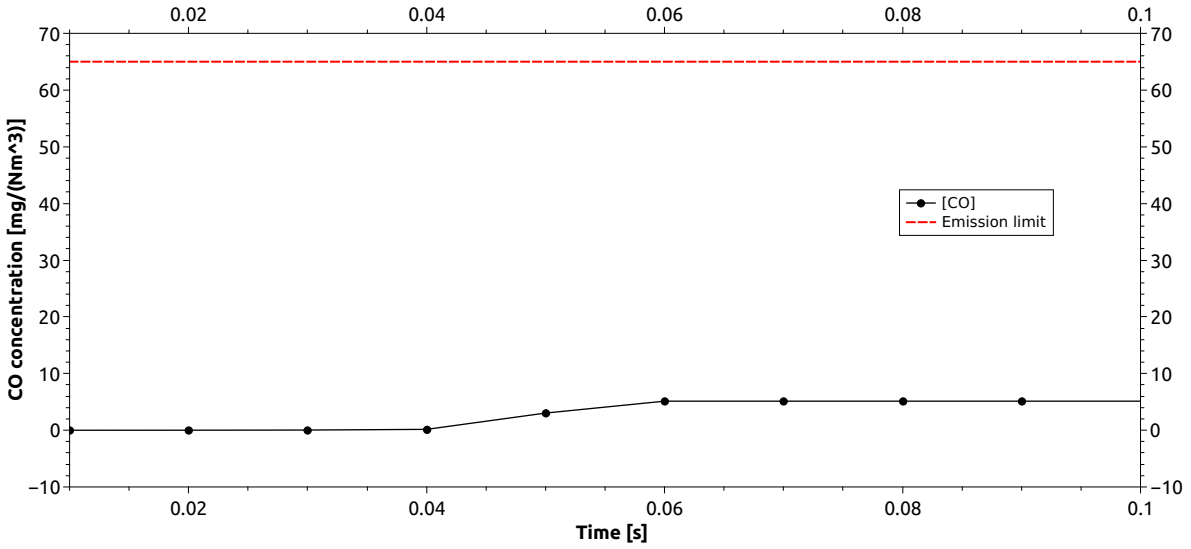

Figure 10. CO concentration during the combustion reaction.

4 Concluding remarks

Based on the present analysis, the results differences are noticible when combustion has been taken into account in the Brayton cycle instead of pure air as working fluid. The combustion model might present overestimated values since not all losses from the combustion reaction were modelled. Independently from the losses modelling, when comparing the own model (10-equation system) buitl in Scilab© and the one from the chemFoam solver (hundreds-equation system), the molar fraction of the combustion products varies from 0.76 to 45.39 %. Thus, considering only the main combustion products in the model may not be enough to represent the products molar fractions. Regarding the emission control polluents, both models predicted CO and NO levels below the the ones defined by the local regulatory authority (CONAMA).

References

[1] Lora, E. E. S., Nascimento, M. A. R., et al., 2004. Geração termelétrica: planejamento, projeto e operação. *Rio de Janeiro: Interciência*, vol. 1, pp. 2.

[2] Branco, F. P., 2005. Análise termoeconômica de uma usina termelétrica a gás natural operando em ciclo aberto e em ciclo combinado. *Ilha Solteira, São Paulo: Universidade Estadual Paulista. Dissertação (Mestrado Engenharia Mecânica), Programa de Pós-Graduação da Faculdade de Engenharia de Ilha Solteira da Universidade Estadual Paulista*.

[3] Queiroz, M. & Matias, J. A., 2003. Curso Básico de Turbinas a Gás - Petrobras. http://epe.gov.br/pt. (Accessed June 20, 2019).

[4] Ferguson, C. R. & Kirkpatrick, A. T., 2015. *Internal combustion engines: applied thermosciences*. John Wiley & Sons.

[5] Ziółkowski, P., Zakrzewski, W., et al., 2013. Thermodynamic analysis of the double brayton cycle with the use of oxy combustion and capture of CO2. *Archives of thermodynamics*, vol. 34, n. 2, pp. 23–38.

[6] Olikara, C. & Borman, G. L., 1975. A computer program for calculating properties of equilibrium combustion products with some applications to IC engines. Technical report, SAE Technical Paper.

[7] Maioli, A. et al., 2016. CFD OpenFOAM: Implementação da combustão smouldering e sua avaliação paramétrica. Master's thesis, Universidade Federal do Espírito Santo.

[8] Moran, M. J., Shapiro, H. N., & Boettner, D. D., 2000. *Princípios de termodinâmica para engenharia* . Grupo Gen-LTC.

[9] CETESB, E. Q., 2016. Ficha de informação de produto químico. https://sistemasinter.cetesb.sp.gov.br/produtos/ficha_completa1.asp?consulta=METANO. (Accessed June 20, 2019).

[10] Gama, G., 2016. Propriedades dos gases. http://www.gamagases.com.br/propriedades-dos-gases-metano.html. (Accessed June 20, 2019).